JOURNAL OF THERMOPHYSICS AND HEAT TRANSFER
Vol. 17, No. 2, April–June 2003

Capillary Pumped Loop Startup: Effects of the Wick Fit on Boiling Incipience

Vincent Dupont*
Swiss Federal Institute of Technology, CH-1015 Lausanne, Switzerland
and
Jean L. Joly,† Marc Miscevic,† and Vincent Platel†
Université Paul Sabatier, 31062 Toulouse Cedex, France

The onset of boiling in a capillary pumped loop evaporator is experimentally studied. The evaporator of the system contained a porous material in which the working fluid (n-pentane) was vaporized. The system was started up with the evaporator completely flooded, and boiling was initiated by application of a heat load. A specific flat plate evaporator was designed where the distance between the heating plate and the wick can be controlled. The two parameters studied were confinement and power applied (600 W maximum). The superheat needed to initiate boiling was strongly dependent on the quality of the contact between the heating plate and the wick and on the power applied. The initial superheat played a decisive role in the behavior of the system at startup. From the beginning, there were strong couplings between the physical phenomena occurring in the evaporator and the reservoir.

Nomenclature

e	=	confinement, μm
L_v	=	latent heat of vaporization, $J \cdot kg^{-1}$
M	=	molecular weight, $kg \cdot mol^{-1}$
P	=	pressure, Pa
Q	=	power, W
R	=	universal gas constant, $J \cdot mol^{-1} \cdot K^{-1}$
r	=	pore radius, m
T	=	temperature, °C
σ	=	surface tension, $N \cdot m^{-1}$

Subscripts

c	=	critical
cond	=	condenser
evap	=	evaporator
hp	=	heating plate
i	=	incipience
in	=	inlet condition
isol	=	isolator
l	=	liquid
out	=	oulet condition
p	=	pore
res	=	reservoir
sat	=	saturation
sec	=	secondary fluid
vap	=	vapor phase

Introduction

HEAT fluxes generated by electronic chips in telecommunications satellites and orbital stations are constantly increasing, and the distances between these heat sources and the radiative panels are also growing. These considerations have encouraged the space industry to develop capillary pumped loop (CPL) technology[1] to replace the conventional thermal management systems (heat pipes, etc.). CPLs allow large heat loads to be transferred between sources that can be tens of meters apart.

These systems need no mechanical pumping; they use the properties of the liquid–vapor phase change phenomena inside a porous wick to move the fluid and, thus, to transport heat. Such systems have been intensively studied since the 1980s and are now becoming available for practical use. For instance, in the French demonstrator satellite Stentor, a CPL provides thermal control[2] for the transmitting active antenna.

The behavior of a CPL in steady state is well known. Therefore, researchers are now investigating the transient regime of these systems, in which most of the problems come from hydrodynamic oscillations and the evaporator startup. At startup, the loop is completely flooded with liquid, and heat flux is applied to the metallic body of the evaporator. The temperature of the liquid rises until it reaches the boiling incipience superheat value[1] $\Delta T_{sat,i}$. Published works on CPL startups are limited. Table 1 summarizes the incipience startup superheat values available in the literature.[3–13] When $\Delta T_{sat,i}$ was not specified in the reference, it was taken from the evaporator body temperature curves. In the same way, when not indicated, the heat flux applied at startup was calculated from the heat power applied and the geometrical characteristics of the evaporator.

Cullimore[14] notes the various problems that can arise when a CPL is started up in the flooded state. In particular, he analyzes the onset of boiling and the reaction of the reservoir to the arrival of liquid during the first few moments, as well as the influence of gravity. The incipience superheat in the evaporator $\Delta T_{sat,i}$ is always greater than that observed under steady conditions and has a random character. The greater the superheat, the more sudden the emptying of the vapor grooves is. Cullimore suggests that each evaporator has a maximum incipience superheat value, above which the system deprimes. Hoang and Ku[15] point out that the effects of inertia and pressure drops in the lines when the evaporator empties could exceed the maximum capillary pressure difference. In microgravity, menisci in the evaporator grooves disturb the vapor line surge.[16]

Ku[17] has reviewed the state of the art for NASA CPLs startup. The incipience superheats lie between 0 and 6 K for liquid-flooded cylindrical evaporators. He shows that there are two types of startup (Figs. 1a and 1b). The first (Fig. 1a) is "smooth" and occurs with

Received 3 December 2001; revision received 7 August 2002; accepted for publication 14 October 2002.

*Scientific Collaborator, Laboratoire de Transfert de Chaleur et de Masse, Institut des sciences de l'énergie; vincent.dupont@epfl.ch.

†Maitre de conference, Laboratoire d'Etude des Systèmes et de l'Environnement Thermique de l'Homme (LESETH), 118 route de Narbonne.

practically no superheating; the evaporator is primed every time. The second (Fig. 1b) occurs when superheating is high and is followed by a pressure spike which generally results in depriming. Maidanik et al.[18] describe similar behavior in loop heat pipe startup. No explanation is given for the cause of this difference in behavior. Any method that can reduce the incipience superheat increase the chance of a successful startup.[1]

Ku[17] compares the startup behavior of three evaporators differing only by their inner diameters (30, 16, and 14 mm). The small-diameter evaporators showed high superheat at startup, which consistently led to depriming. Surface treatments applied to the inside walls of these evaporators did not reduce $\Delta T_{\text{sat},i}$. The 30-mm-diam evaporators started up smoothly. Ku deduces that evaporator size influences the superheat at the incipience of boiling. Pohner and Antoniuk,[19] on the other hand, assert that boiling only depends on microscopic variables and that the problem is more likely to be due to the presence of noncondensable gases. Mo et al.[13] showed a startup time reduction in a CPL enhanced by an electrohydrodynamic (EHD) technique, for small heat flux. Our own experience at LESETH[20] has previously shown that, for identical evaporators, a tightly fitting wick consistently led to depriming, whereas the problem could be avoided with a looser fit. To solve these operating problems, a capillary starter pump has been developed at NASA.[1] It is a self-priming evaporator that is used to clear out the liquid present in the vapor grooves and lines of the main evaporator. Such a solution seems to be effective, but it increases system complexity and reduces compactness. The time necessary to start the loop is also significantly increased.[13] Another solution to increase the reliability of CPLs is to assist startup with mechanical pumping.[6,7]

The study presented in this paper was performed with the intention of identifying and understanding the physical phenomena connected with the incipience of boiling in the CPL evaporator and its influence on the control reservoir. We chose to pay particular attention to the role of the confinement, which represents the distance separating the wick from the metallic body of the evaporator. A special flat plate evaporator was designed to study the few seconds after the boiling incipience instant. The material used, as well as the elementary geometry of the region between the heating plate and the wick, were expected to be representative of those of an operational CPL evaporator. The design of this evaporator is not suitable for operational use as discussed in the "Results" section. A possible explanation for the two kinds of startup behavior will be given.

Table 1 Observed values of surperheat and depriming ratio at startup

Device	Year	Fluid	φ, kW/m^2	$\Delta T_{\text{sat},i}$, K	Check	Reference
CPL breadbord	81	R-11	3–22		Yes	3
CPL1	84	NH_3	2–9		1/12	4
CPL/GAS	85	NH_3	2–8	1–3.5	Yes	4
CPL2	85	NH_3	2–9		No	4
CPL/Hitchiker	86	NH_3	6–27		4/7	5
Model M2	90	NH_3			Yes	6
CAPL-1	94	NH_3			58/84	7
WCHP	94	NH_3		2–6	Yes	8
Dornier	95	NH_3	1.8	4.5		9
CAPL-2	96	NH_3	0.6–7	1–6.7	No	10
BFDPT	96	H_2O	11.2–56	0–4.5		9
BFDPT	97	R-134a	2–14	3–8.5		11
CAPL-3	97	NH_3	3.6	7	No	12
EHD CPL	99	R-134a	0.3–1.6	0.2–0.8	No	13

Experimental Apparatus

A flat plate evaporator was designed and manufactured in which the distance between the upper surface of the wick and the grooved surface of the heater plate was controlled (variable confinement). Particular attention was paid to the visual display. Visualization constraints and the possibility of movement of the wick have involved an important oversizing and an increase of thermal mass of the evaporator. As shown in Fig. 2, the CPL components were the plane evaporator, a condenser, an isolator, and a control reservoir linked together with either rigid or flexible transparent pipes. As working fluid, n-pentane was chosen to compare results with previous boiling incipience studies.[21]

Flat Plate Evaporator

The evaporator, symmetrical under revolution, was designed around a porous disk that constituted the wick (Fig. 3). The liquid entered the evaporator through the liquid inlet area 1, i.d = 150 mm, $h = 60$ mm, then crossed the wick, where it was vaporized. The vapor was guided by squared striations and eight rounded grooves toward the vertical outlet, the outlet bend, and the vapor line. The heater plate could be considered as 1024 aluminium alloy disk. Its diameter was 154 mm and its thickness 15.4 mm. The grooves and striations network was machined in the heating plate (Fig. 4).

It formed the upper part of the body of the evaporator. Its top face was in contact with the heating element (Fig. 3), which was an electrical resistance providing up to 600 W of power. To reduce the losses, the heater was insulated on the top. The evaporator was instrumented with 17 K-type 0.5-mm thermocouples arranged parallel to the radius of the heater plate (perpendicular to the thermal gradient). Thermocouple uncertainty was 0.2°C. A differential pressure transducer gave the pressure difference ΔP_{evap} between the evaporator inlet and outlet (Fig. 2). Its measuring range was ±5000 Pa with an accuracy of 25 Pa.

Porous Wick

The wick (Fig. 3) was a flat porous disk, 120 mm in diameter and 6.4 mm thick, composed of sintered Pyrex® particles. The material choice criteria were the mechanical rigidity, planeness of the face in contact with the heating plate, small dispersion of pore sizes around the average (uniformity), and low thermal conductivity. The average pore radius, determined by mercury porosimetry, was 8.5 μm

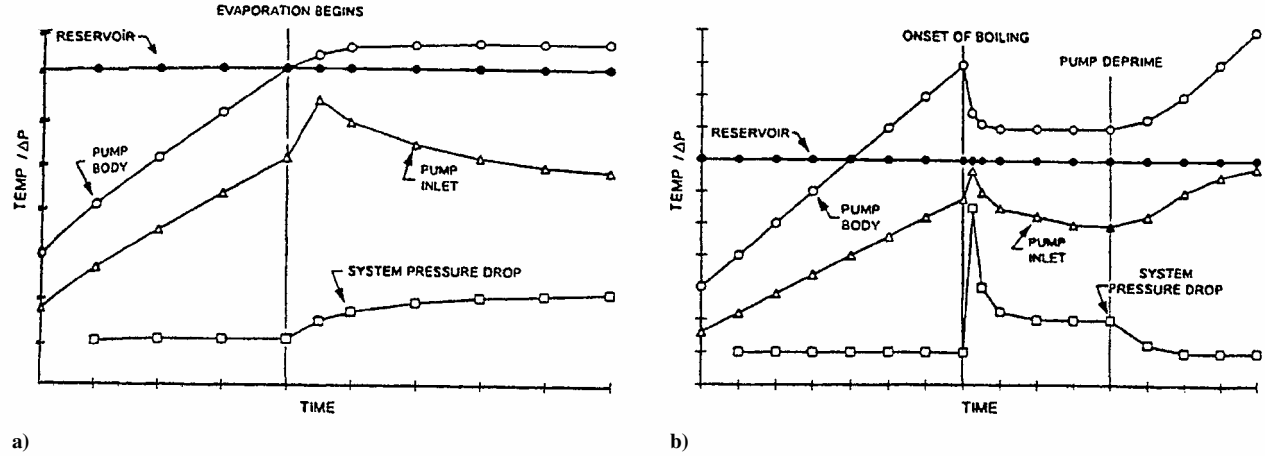

Fig. 1 Two types of CPLs startup in fully flooded conditions (Ku[1]).

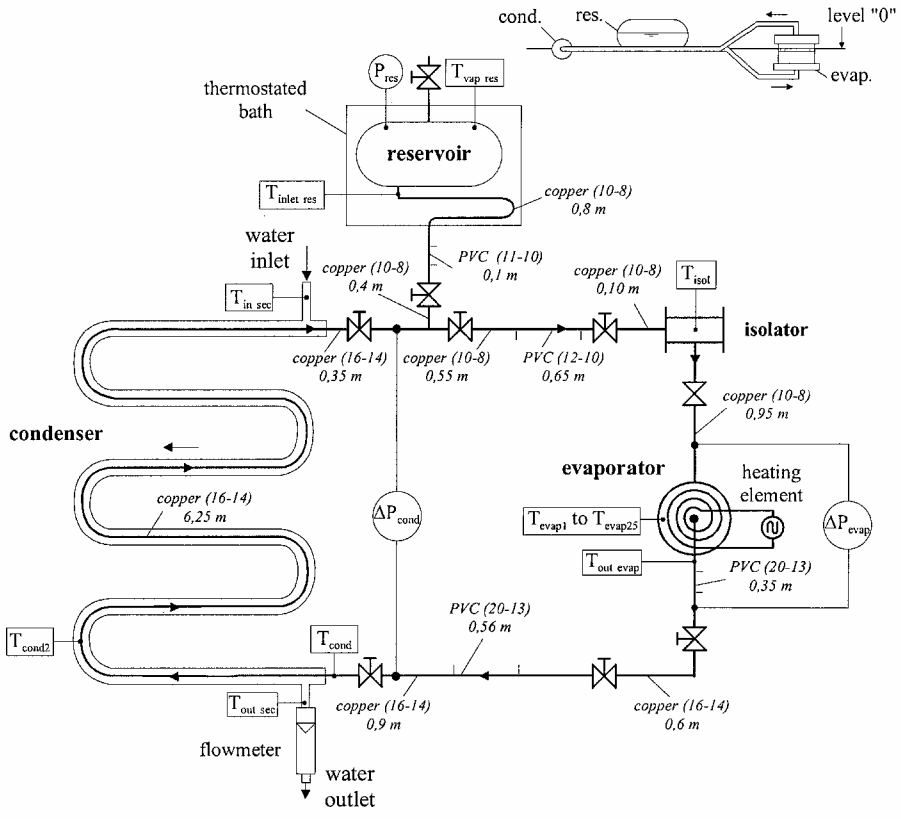

Fig. 2 Schematic of the CPL, between brackets: outer and inner diameters of the lines, in millimeters.

and the permeability κ was 4×10^{-13} m^2. The support-wick assembly formed a porous piston, which was fixed to a vertical rod 10 (Fig. 3) that moved with a micrometer screw. The piston could move a maximum distance of 2 mm. The variable distance e between the upper surface of the wick and the lower surface of the heater plate, at the base of the striations and grooves, was the main parameter of this study. There was some play in this device that was difficult to estimate and that led to a variation in e over the contact area. In particular, the wick upper surface was not perfectly flat and has undulations of an amplitude of 70 μm. For this reason, only two extreme positions (0 and 1400 μm) are presented. Of course, a confinement of 1400 μm is not representative of the wick fit in an operationnal CPL evaporator; this value was taken for demonstration purposes only.

Control Reservoir

The 2.5-liter reservoir was composed of a horizontal hollow, steel cylinder (i.d. 110 mm and length 240 mm), immersed in a bath at an operational temperature set (close to 41°C) to within 0.1 K by a thermocryostat. The liquid–vapor interface in the reservoir fixed the saturation conditions in the CPL. Three thermocouples measured the temperatures in the vapor phase, reservoir inlet, and thermostated bath with an uncertainty of 0.2°C. An absolute pressure sensor measured the vapor pressure P_{res} with an accuracy of 250 Pa. The vertical location of the liquid surface in the reservoir varied during startup. The elevation difference between this liquid surface and the main horizontal plan of the loop varied from 0 to 20 mm.

Condenser

The condenser was composed of two coaxial tubes. The working fluid circulates in the inner tube and cooling water circulates in the opposite direction in the secondary circuit. The countercurrent water flow rate in the secondary circuit was set at 256 l · h^{-1} and the temperature at 18°C. The condenser was oversized (6 m long) to ensure good liquid subcooling. The inlet and outlet condenser axes were in the same horizontal plane as the lower surface of the heating plate.

Test Procedure

Nucleation in a superheated fluid creates strong dynamic phenomena in the loop, which necessitate the use of a fast acquisition system. In the studies reviewed in the Introduction, such fast systems were not used because the technology was not available or experiments were made over long times (order of magnitude of 1 h). In the present study, acquisition was performed at a rate of 100 samples/s averaged over 10 samples, thus giving 10 acquisitions/s. All of the results reviewed in Table 1 were obtained with a too slow acquisition speed (several minutes), unsuitable for the accurate study of the boiling incipience phenomena. The two control parameters studied were the applied power Q and the confinement e. This was not a parametric study but rather an attempt to demonstrate the influences of the confinement and thermal load on system behavior. The relatively random behavior associated with boiling incipience[22–24] obliged us to make 4–30 tests per pair of parameters e and Q.

Results

Figure 5 shows the time variation of the heating plate superheat for applied powers of 200 and 600 W and confinement values of 0 and 1400 μm. The Fig. 5 curves have been time shifted to obtain the same origin at boiling incipience. This particular time was determined by the first slope change in 1 of the 17 temperature evolutions of the thermocouples placed in the heating plate. Video camera observations confirm the relation between slope change and fast bubble formation in the groove.

For the sake of clarity, the temperature of the heating plate is illustrated by the variations of a single representative thermocouple $\Delta T_{sat,i} = T_{hp} - T_{sat}$; the saturation temperature is the temperature of the vapor phase in the reservoir (~41°C). Heating plate temperature evolution during the startup was similar to the descriptions[1,13,14,17] in previous studies for cylindrical evaporator design. At $t < 0$ s, there is a transient conduction regime in the fully flooded evaporator, the temperatures increases are nearly linear, involving liquid superheating. At $t = 0$ s, the boiling incipience superheat $\Delta T_{sat,i}$ is reached, and a vapor phase appears suddenly in the evaporator. The boiling process takes a considerable amount of energy from the plate, which

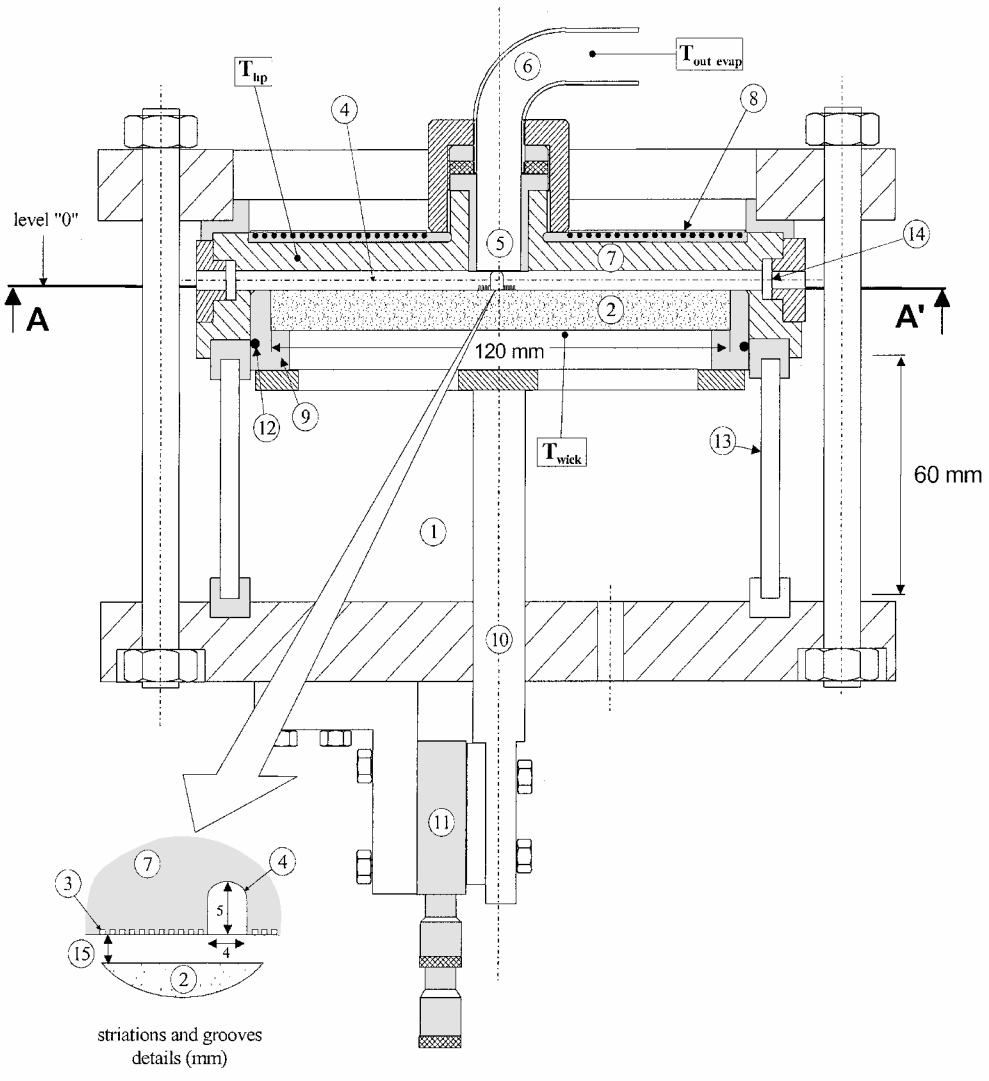

Fig. 3 Cross-sectional view of the evaporator: 1) liquid inlet area, 2) wick (sintered Pyrex), 3) striations (0.5 × 0.5 mm^2), 4) groove, 5) vertical outlet (PTFE), 6) vapor outlet bend (copper), 7) heating plate (AU4G), 8) heating element (brass), 9) wick suport (PTFE), 10) translation rod, 11) micrometric screw, 12) quadrilobe sealing (Viton), 13) transparent tube (Pyrex), 14) window (Pyrex), and 15) confinement *e*.

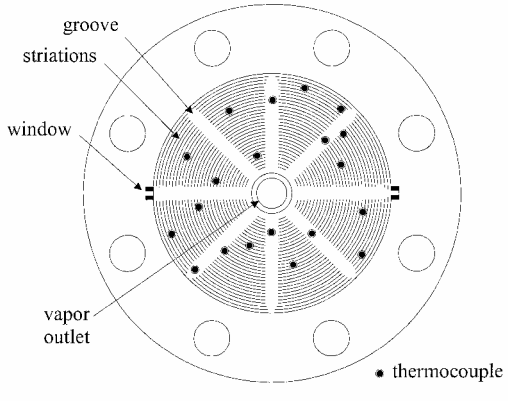

Fig. 4 Striations and grooves pattern of the downward face of the heating plate, with the location of the thermocouples and observation windows (A'A view of Fig. 3).

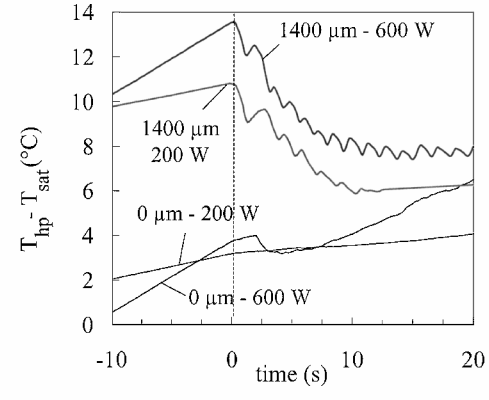

Fig. 5 Plate superheat evolution with *Q* at 200 and 600 W and *e* at 0 and 1400 μm.

explains the slope change. The phase at $t > 0$ s corresponds to the liquid purge from the grooves and "vapor line." Phase change phenomena increase heat transfer inside the evaporator, and the plate temperature drops.

Two types of behavior can be distinguished, directly determined by the confinement value.

For $e = 1400$ μm, the heating plate superheat at the onset of nucleate boiling is over 10°C; the following temperature drop is large and so the instant when the slope change occurs is easy to determine. The scalloped aspect of the curves (Fig. 5) is directly connected with wetting–drying events observed visually in the grooves. Because of the thermal resistance of the vapor layer, for such confinements, the evaporator should deprime quickly. However, the wetting–drying events caused by oscillations in the loop maintains stable operation for a few minutes.

For $e = 0$ μm, incipience superheat values are within the 2–4°C range, and the slope change (Fig. 5) is less marked. For a

large confinement value, incipience occurs successively in various nucleation sites. This behavior leads to greater dispersion and uncertainty on $\Delta T_{\text{sat},i}$. Because of this relative dispersion, the minimum, $\Delta T_{\text{sat},i,\min}$, and maximum, $\Delta T_{\text{sat},i,\max}$, superheat values for each single startup test are noted rather than a mean value. These two representative types of startup are comparable to the smooth and violent startup described by Ku[1] (Fig. 1). In our configuration, confinement could explain this behavior as will be discussed.

In the curves (Fig. 5), one could note a rise of the temperature of the heating plate after the boiling incipience. In fact, in both cases the evaporator deprimes several minutes after the beginning (vapor appearance under the wick). The particular design of the evaporator could explain this behavior. The main possible reasons for the deprime of the present study loop are the high values of the thermal inertia of the heating plate and of the important amount of liquid under the wick, as well as the penetration of vapor in the sealing between the support of the wick and the porous media. Remember that only the value of the boiling incipience superheat and the loop behavior in the few seconds after incipience were studied; other works in the literature[1,14,17] had already proved the link between high boiling incipience superheats and deprime.

Confinement Influence

Figure 6 is a plot of the average maximum superheating at boiling incipience vs e parameter for $Q = 200$ W. Each point, e and Q, is the average of 4–30 single startup tests. The error bars correspond to 95% confidence intervals calculated from Student statistic law. The error bars show the dispersion and take the number of samples into account. (The large error bars for 1000 μm are due to a small number of experiments.) Two types of incipience superheat can be seen, directly related to confinement:

$$e > 1000\ \mu\text{m} : \Delta T_{\text{sat},i,\max} > 10.1^\circ\text{C}$$

$$e < 500\ \mu\text{m} : \Delta T_{\text{sat},i,\max} < 4.2^\circ\text{C}$$

There is a confinement threshold, of the order of 1 mm for this evaporator, which marks the limit between the two types of behavior. The same conclusions can be drawn from the minimum superheat values.

Heat Flux Influence

Figure 7 is a plot of the variations of the mean maximal and minimal incipience superheat vs Q, for values of e equal to 0 and 1400 μm. Each point is the mean of 5–21 tests. The error bars correspond to 95% confidence intervals (Student law). The quality of the contact between the porous wick and the inside wall of the evaporator has a major influence on the level of superheating when boiling occurs. Two clearly separated groups of boiling incipience superheat appear:

$$e = 1400\ \mu\text{m} : 7.4\ \text{K} < \Delta T_{\text{sat},i} < 15.8^\circ\text{C}$$

$$e = 0\ \mu\text{m} : 1.8\ \text{K} < \Delta T_{\text{sat},i} < 5.2^\circ\text{C}$$

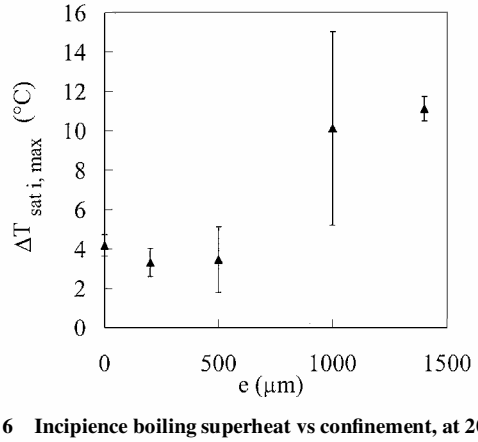

Fig. 6 Incipience boiling superheat vs confinement, at 200 W.

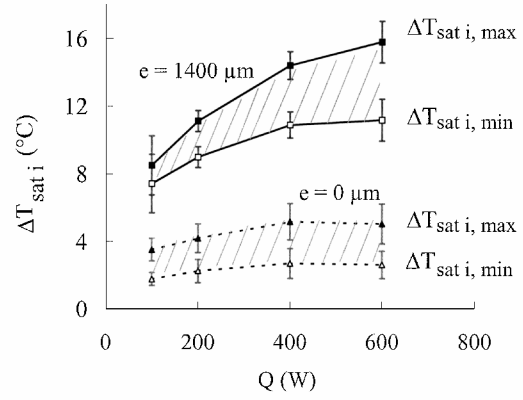

Fig. 7 Incipience boiling superheat vs heat flux.

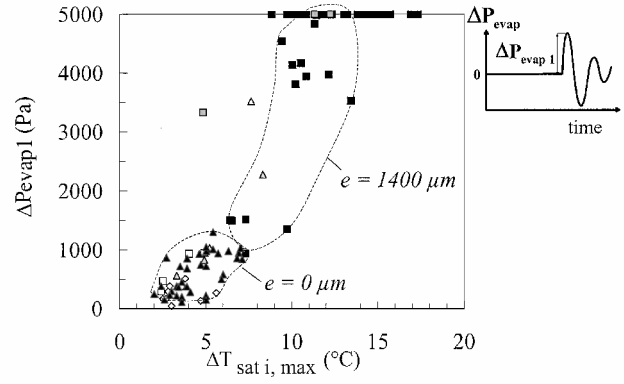

Fig. 8 First pressure spike vs maximum incipience superheat: ■, $e = 1400$ μm; ▣, $e = 1000$ μm; □, $e = 500$ μm; ◇, $e = 200$ μm; △, $e = 150$ μm; ▲, $e = 80$ μm; and ▲, $e = 0$ μm.

This behavior is consistent with the existence of a confinement threshold. The curves (Fig. 7), in particular for $e = 1400$ μm, show a certain dependence of $\Delta T_{\text{sat},i}$ on the applied heat flux: the maximum superheat is nearly doubled when the power goes from 100 to 600 W.

Temperature Variations Under the Wick

As Cullimore[14] notes, at the onset of boiling, the liquid leaves the evaporator by the vapor outlet but also through the wick and out of the "liquid inlet." In our apparatus, this was expressed by an abrupt rise in the temperature under the wick, T_{wick}, followed by a fall corresponding to the sucking of cold liquid into the wick. The maximum increase in T_{wick} at incipience was between 0.3°C for $e = 0$ μm and 4 K for $e = 1400$ μm. We never observed visually bubble formation under the wick at startup; T_{wick} never reached T_{sat}, even for the highest superheats. The wick was thick and not very permeable, and the vapor front never managed to cross the porous medium in the way suggested by Cullimore. For thinner wicks such as those used in small-diameter cylindrical evaporators, this crossing is a possibility.

Differential Pressure Variations at the Evaporator

Following the onset of nucleate boiling, two-phase flow occurs between the evaporator and the condenser. Mass flow rate and ΔP_{evap} oscillations characterize this transient phase. Figure 8 shows the variation of the amplitude of the first differential pressure spike ΔP_{evap1} vs $\Delta T_{\text{sat},i,\max}$ for various confinement values. The results correspond to approximately 100 startups. Because the measurement range of the pressure sensor was restricted to 5 kPa, the results of the most violent tests are truncated. The envelopes correspond to tests using extreme values of confinement ($e = 1400$ and 0 μm). Although there is some dispersion of the values, it is clear that the initial pressure spike tends to increase when the superheat required to start boiling increases. Our results agree with Cullimore's[14] and Ku's[17] analyses, which associate the intensity of the strongly dynamic regime with the superheat values at incipience. Notice that,

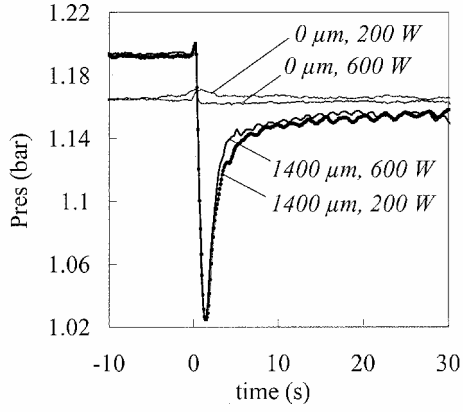

Fig. 9 P_{res} vs t for confinement values of 0 and 1400 μm and power values of 200 and 600 W.

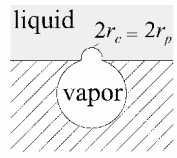

Fig. 10a Vapor nucleus trapped in a spherical cavity.

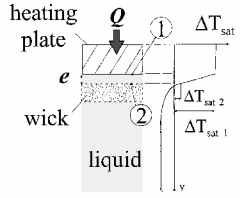

Fig. 10b Temperature profile in the evaporator during startup.

if the porous body is not able to absorb this abrupt pressure spike, the evaporator could deprime.

Figure 9 shows the time variation of P_{res} for four representative tests corresponding to confinement values of 0 and 1400 μm and powers of 200 and 600 W. Consequent to incipience of nucleate boiling, liquid is forced out of the evaporator toward the reservoir by the vapor expansion. The confinement value determines the type of $P_{res}(t)$ behavior.

For $e = 0$ μm, there is practically no reaction in the reservoir, and the startup is smooth. For $e = 1400$ μm, P_{res} is seen to rise by about 100 Pa for 0.8 s, which corresponds to the arrival at the reservoir inlet of the liquid contained in the immersed coil, at T_{sat}. In a second phase, P_{res} falls by 16 kPa before rising asymptotically as the reservoir returns to its reference temperature. The arrival of cold liquid from the pipes that were initially at ambient temperature or from the condenser creates a cold shock. This phenomenon changes the saturation conditions in the system as a whole. Note that the liquid–vapor system in the reservoir is at the saturation conditions, $P_{res} = P_{sat}$ ($T_{vap\,res}$), even during the strongly transient phase. Depriming due to the cold shock was not observed in our system. The heat and mass transfers between the reservoir and the rest of the loop at startup cannot be dealt with here. Nevertheless, this example illustrates the harmful consequences of high superheats when boiling starts in the evaporator and the coupling that exists between the evaporator and the reservoir in the first few seconds of CPL operation.

Discussion

The activation process of boiling, homogeneous, heterogenous, or by nucleation of preexisting vapor nuclei, is driven by microscopic-scale phenomena in superheated liquid, which is associated with the notion of boiling incipience superheat. In the CPL evaporator, boiling starts from preexisting vapor nuclei trapped in surface cavities or cracks: the nucleation sites. These sites exist on every solid wall: the heating plate 1 and the porous wick 2 (Fig. 3). A site can be activated if it is able to trap and keep a vapor embryo during the phases before startup when the evaporator is fully flooded and subcooled. Reservoir-type cavities such as a spherical cavity (Fig. 10a) best satisfy the equilibrium condition and stability criterion.[25] Because of their high wettability, cooling fluids easily fill cavities having large diameters and/or openings over wide angles. Only vapor embryos of small radius are likely to be activated. The activation superheat of a site depends on its geometry and the thermophysical properties of the fluid and the wall. For each site there is a critical radius r_c for the vapor embryo above which its growth will be unstable. If the superheat is small by use of Clapeyron's relationship and the assumption that the vapor is a perfect gas, the superheat and critical radius can be shown to be determined by the equation[22]

$$\Delta T_{sat} \cong (2\sigma/r_c)(R/L_v M)\left(T_{sat}^2/P_l\right)$$

For example, in the case of a spherical cavity, r_c is the pore mouth radius.[25] In practice, incipience boiling superheat on real surface is difficult to predict because of the diversity of microgeometry, hysteresis in the contact angle,[23] and the influence of the thermal history of the plate before activation.

The preceding results show two startup types, smooth or violent, directly correlated with boiling incipience magnitude, an observation consistent with thoses of the literature.[1,14,18] In our case, the difference in behavior, controlled by incipience boiling superheat, was essentially connected to the confinement value. That the behavior was specific to each evaporator encourages us to link smooth and violent startup types to the onset of boiling in the porous medium and on the body surface of the evaporator, respectively (Fig. 10b). The porous wick had a structure obtained by sintering particles that create easily activatable reservoir-type cavities. Incipience superheats associated such a structure are moderate, of the order of 1°C. The metal heating plate surface presented smaller cavities than the wick and $\Delta T_{sat,i} \approx 10$°C. As shown by Fig. 10b, when heat load was applied on the external evaporator wall, a transient conduction regime occurred in the various layers of the evaporator and, possibly by convection, in the grooves and the gap. For $e = 0$ μm, boiling started on the upper face of the wick. When the wick and plate were slightly separated, heat transfer through the thickness of the superheated liquid still allowed boiling incipience on the wick, but beyond a certain threshold thickness, boiling appeared on the heating plate with a high superheat. This scenario is consistent with the experimental confinement threshold and with previous results found in a study on boiling incipience in an elementary horizontal confined space[21] made with the same materials and fluid. This study clearly shows that the two types of startup are related to nucleation sites location and/or their ability to be activated. This conclusion could explain the failure, pointed out by Ku,[17] to reduce $\Delta T_{sat,i}$ by means of the usual surface treatments (sanding or corrugation) applied to the heating plate. The superheat values (Table 1) indicate that nucleation occurs on the wick in the NASA cylindrical evaporator and decreasing $\Delta T_{sat,i}$ would depend on an improvement of the vapor trapping and holding capabilities of the wick. This goal could be reached by creating reservoir-type cavities with a suitable mouth radius and/or decreasing wick material wettability [with a PTFE (Teflon®) layer for example]. This wick surface enhancement would not have to be applied to the whole porous wick because there is a risk of increasing the depriming sensitivity of the evaporator. You et al.[24] and Liang and Yang[26] propose solutions to reduce superheat at boiling incipience, but these appear difficult to use in the case of a CPL evaporator. The EHD effect on incipience superheat is not yet clear.[13]

The dependence of $\Delta T_{sat,i}$ on the heat flux is rarely mentioned in the literature and cannot be explained by the conventional theory of boiling.[24] It seems that there is a delay time of about 1 s in the boiling process activation for strongly dynamic regimes, and this entails an increase in the superheat at incipience. This dependence has been demonstrated by Nghiem et al.[27] for heterogeneous boiling configurations, but the origin of the delay remains unexplained for nucleate boiling for the time being. In a practical sense, this dependence cannot be neglected.

In our experiments, the presence of a variable gap was only motivated by the determination of the localization of the vapor nuclei activated at startup. In other studies such a gap, of 10 μm of order of magnitude, was recommended[9,19,20,28] to lower vapor pressure drop in the wick. The presence of this liquid layer between the wick and the heater plate has several effects: It increases the superheat necessary for boiling incipience, it increases the volume of superheated liquid in which the vapor front develops, and it plays a role in the organization of the flow when liquid is expelled from the evaporator (pressure drops and inertia). The onset of boiling in a large volume of superheated liquid is explosive and is expressed by an abrupt pressure rise. This rise is moderate when the liquid is confined in the porous body; the menisci press on the solid structure of the wick, thus, tempering the violence of the vaporization.

The differential pressure ΔP_{evap} measures pressure drops and the effect of acceleration of the liquid and/or vapor in the wick and the grooves and also any capillary pressure jump resulting from front penetration in the wick. The maximum capillary head developed by the wick with n-pentane as the working fluid was 3200 Pa. The variations of ΔP_{evap} can be seen to be greater than this maximum pressure jump, which tends to confirm the penetration of the vapor into the porous medium. An analysis of the movement of the fluid in the vaporization area following boiling incipience would necessarily require fine modeling of these phenomena.

Conclusions

This study has highlighted the importance of boiling incipience superheat related with the confinement between the porous wick and the heater plate when a CPL starts up under fully flooded conditions. The influence of heat flux has been studied at the same time.

A specific experimental setup has been presented that allows the space between the heating surface of a plane evaporator and the porous wick to be varied. The experimental results show that the nucleation starts in two different ways.

One is smooth and corresponds to low superheats at boiling incipience ($1.8 < \Delta T_{\text{sat},i} < 5.2^{\circ}$C). This occurs when confinement is strong ($e = 0$ μm). In this case boiling starts on the wick.

The other is violent and corresponds to high superheats at the start of boiling ($7.4 < \Delta T_{\text{sat},i} < 15.8^{\circ}$C). This occurs when confinement is weak ($e = 1400$ μm). In this case boiling starts on the heating plate.

The two types of onset of boiling correspond to those observed for cylindrical evaporators, but the localization of the nucleation sites on the porous wick is a new step in the understanding of the CPL startup. This study shows that wick fit is a new parameter to take into account in the analysis of the CPL startup. Through its influence on $\Delta T_{\text{sat},i}$, confinement played a particularly important role in the startup phase of our device. One important conclusion is that a too loose fit of the wick in the evaporator body could lead the CPL to deprime.

The heat flux has a nonnegligible influence on the boiling incipience superheat in the capillary evaporator, but for reasons that are yet unclear. Particular attention should, therefore, be paid to how the thermal load is applied to the evaporator when the system is started up.

Thus, it would appear wise to choose a porous medium in which the side in contact with the heater plate is the most capable of trapping and holding vapor embryos. This characteristic may possibly be in contradiction with the constraints on pressure drop in the wick.

Acknowledgments

This work has been granted by the French Ministry of Education and Research. The authors acknowledge Claude Butto for the initiation of this project.

References

[1]Ku, J., "Recent Advances in Capillary Pumped Loop Technology," *Proceedings AIAA National Heat Transfer Conference*, AIAA, Reston, VA, 1997, pp. 1–21.

[2]Curbelie, B., and Ehster, B., "Stentor Programme: An Ongoing and Efficient Way for Preparing the Future," *Acta Astronautica*, Vol. 44 , No. 7–12, 1999, pp. 709–716.

[3]"Capillary Pump Loop (CPL) Heat Pipe Development Status Report," NASA CR-175273, 1982, pp. 1–39.

[4]Ku, J., Kroliczek, J., Butler, D., Schweickart, R. B., and Mcintosh, R., "Capillary Pumped Loop GAS and Hitchhiker Flight Experiments," *Proceedings of the 4th AIAA/ASME Joint Thermophysics and Heat Transfer Conference*, AIAA, New York, 1986, pp. 1–11.

[5]Ku, J., Kroliczek, J., and Taylor, W. J., "Functional and Performance Tests of Two Capillary Pumped Loop Engineering Models," *Proceedings of the 4th AIAA/ASME Joint Thermophysics and Heat Transfer Conference*, AIAA, New York, 1986, pp. 1–11.

[6]Wulz, H., and Embacher, E., "Capillary Pumped Loop for Space Applications: Experimental and Theoretical Studies on the Performance of Capillary Evaporator Designs," AIAA Paper 90-1739, 1990, pp. 1–16.

[7]Butler, D., Ottenstein, L., and Ku, J., "Flight Testing of the Capillary Pumped Loop Flight Experiment," *SAE Transactions*, Society of Automotive Engineers, Warrendale, PA, 1995, pp. 750–764.

[8]Antoniuk, D., and Pohner, J., "Deleterious Effects of Non-condensible Gas During Capillary Pumped Loop Start-up," *SAE Transactions*, Society of Automotive Engineers, Warrendale, PA, 1994, pp. 1–11.

[9]Lefriec, C., "Analyse du fonctionnement des boucles diphasiques à pompage capillaire menée par expérimentation d'une boucle à eau," Ph.D. Dissertation Univ. de Poitiers, Poitiers, France, 1997.

[10]Yun, S., Nguyen, T. N., Kroliczek, E., Chalmers, D. C., and Fredley, J., "Design and Ambient Testing of the Flight Starter Pump Cold Plate," *SAE Transactions*, Society of Automotive Engineers, Warrendale, PA, 1996, pp. 1–10.

[11]Dupont, V., Joly, J. L., Miscevic, M., Butto, C., and Platel, V., "Etude du déclenchement de l'ébullition lors de l'amorçage d'une boucle fluide diphasique à pompage thermocapillaire," *Proceedings of the IV Colloque Interuniversitaire Franco-Quebéquois, Systèmes à températures modérées*, Université Laval, Cité Universitaire, Quebec, Canada, 1999, pp. 309–314.

[12]Ku, J., Ottenstein, L., Cheung, K., Hoang, T., and Yun, S., "Ground Tests of Capillary Pumped Loop (CAPL 3) Flight Experiment," *SAE Transactions*, Society of Automotive Engineers, Warrendale, PA, 1998, pp. 1036–1046.

[13]Mo, B., Ohadi, M. M., Dessiatoun, S. V., and Cheung, K. H., "Startup Time Reduction in an Electrohydrodynamically Enhanced Capillary Pumped Loop," *Journal of Thermophysics and Heat Transfer*, Vol. 33, No. 1, 1990, pp. 105–117.

[14]Cullimore, B., "Startup Transient in Capillary Pumped Loops," AIAA Paper 91-1374, 1991.

[15]Hoang, T., and Ku, J., "Hydrodynamic Aspect of Capillary Pumped Loop Systems," *SAE Transactions*, Society of Automotive Engineers, Warrendale, PA, 1996, pp. 1–5.

[16]Butler, D., Ottenstein, L., and Ku, J., "Design Evolution of the Capillary Pumped Loop (CAPL-2) Flight Experiment," *SAE Transactions*, Society of Automotive Engineers, Warrendale, PA, 1996, pp. 1–13.

[17]Ku, J., "Start-up Issues of Capillary Pumped Loop," *Proceedings of the IX International Heat Pipe Conference*, Los Alamos National Lab., Los Alamos, NM, 1995, pp. 994–1001.

[18]Maidanik, Y., Solodovnik, N., and Fershtater, Y., "Investigation of Dynamic and Stationary Characteristics of a Loop Heat Pipe," *Proceedings of the IX International Heat Pipe Conference*, Los Alamos National Lab., Los Alamos, NM, 1995, pp. 1002–1006.

[19]Pohner, J., and Antoniuk, D., "Recent Enhancement to Capillary Pumped Loop Systems," AIAA Paper 91-19314, 1991.

[20]Platel, V., "Etude physique et fonctionnement de l'évaporateur d'une pompe thermocapillaire: modélisation et expérimentation," Ph.D. Dissertation, Univ. Paul Sabatier, Toulouse, France, 1991.

[21]Dupont, V., Joly, J. L., Miscevic, M., Platel, V., and Butto, C., "Etude expérimentale du déclenchement de l'ébullition dans un espace confiné horizontal," *Proceedings of SFT 2000,* Societe Francaise de Thermique, Vandoeuvre, France, 2000, pp. 389–394.

[22]Collier, J. G., and Thome, J. R., *Convective Boiling and Condensation*, 3rd ed., Oxford Science, Oxford, 1994, p. 136.

[23]Tong, W., Bar-Cohen, A., Simon, T. W., and You, S. M., "Contact Angle Effect on Boiling Incipience of Highly-Wetting Liquids," *International Journal of Heat and Mass Transfer*, Vol. 33, No. 1, 1990, pp. 91–103.

[24]You, S. M., Simon, T. W., Bar-Cohen, A., and Tong, W., "Experimental Investigation of Nucleate Boiling incipience with a Highly-Wetting Dielectric Fluid (R-113)," *International Journal of Heat and Mass Transfer*, Vol. 33, No. 1, 1990, pp. 105–117.

[25]Thormählen, I., "Superheating of Liquids at the Onset of Boiling," *Proceedings of the 8th International Heat Transfer Conference*, Vol. 4, Hemisphere, Washington, DC, 1986, pp. 2001–2006.

[26]Liang, H. S., and Yang, W. J., "Nucleate Pool Boiling Heat Transfer in a Highly Wetting Liquid on Micro-Graphite-Fiber Composite Surfaces," *International Journal of Heat and Mass Transfer*, Vol. 41, No. 13, 1998, pp. 1993–2001.

[27]Nghiem, L., Merte, H., Winter, E. R. F., and Beer, H., "Prediction of Transient Inception of Boiling in Terms of a Heterogeneous Nucleation Theory," *Journal of Heat Transfer*, Vol. 103, No. 1, 1981, pp. 69–73.

[28]Figus, C., "Transfert de chaleur et de masse avec changement de phase en milieux poreux, application à l'étude d'un évaporateur capillaire," Ph.D. Dissertation, Inst. National Polytechnique, Toulouse, France, 1996.